



## Lidar observations of marine boundary-layer winds and heights: a preliminary study

Peña, Alfredo; Gryning, Sven-Erik; Floors, Rogier Ralph

*Published in:*  
Meteorologische Zeitschrift

*Link to article, DOI:*  
[10.1127/metz/2015/0636](https://doi.org/10.1127/metz/2015/0636)

*Publication date:*  
2015

*Document Version*  
Publisher's PDF, also known as Version of record

[Link back to DTU Orbit](#)

*Citation (APA):*  
Peña, A., Gryning, S-E., & Floors, R. R. (2015). Lidar observations of marine boundary-layer winds and heights: a preliminary study. *Meteorologische Zeitschrift*, 24(6), 581-589. <https://doi.org/10.1127/metz/2015/0636>

---

### General rights

Copyright and moral rights for the publications made accessible in the public portal are retained by the authors and/or other copyright owners and it is a condition of accessing publications that users recognise and abide by the legal requirements associated with these rights.

- Users may download and print one copy of any publication from the public portal for the purpose of private study or research.
- You may not further distribute the material or use it for any profit-making activity or commercial gain
- You may freely distribute the URL identifying the publication in the public portal

If you believe that this document breaches copyright please contact us providing details, and we will remove access to the work immediately and investigate your claim.

# Lidar observations of marine boundary-layer winds and heights: a preliminary study

ALFREDO PEÑA\*, SVEN-ERIK GRYNING and ROGIER FLOORS

DTU Wind Energy, Risø campus, Technical University of Denmark, Roskilde, Denmark

(Manuscript received July 25, 2014; in revised form April 13, 2015; accepted April 15, 2015)

## Abstract

Here we describe a nearly 1-yr meteorological campaign, which was carried out at the FINO3 marine research platform on the German North Sea, where a pulsed wind lidar and a ceilometer were installed besides the platform's 105-m tower and measured winds and the aerosol backscatter in the entire marine atmospheric boundary layer. The campaign was the last phase of a research project, in which the vertical wind profile in the atmospheric boundary layer was firstly investigated on a coastal and a semi-urban site. At FINO3 the wind lidar, which measures the wind speed up to 2000 m, shows the highest data availability (among the three sites) and a very good agreement with the observations of wind speed and direction from cup anemometers and vanes from the platform's tower. The wind lidar was also able to perform measurements under a winter storm where 10-s gusts were observed above  $60 \text{ m s}^{-1}$  within the range 400–600 m. The ceilometer and wind lidar have also the potential of detecting the marine boundary layer height based on, respectively, direct and indirect observations of the aerosol backscatter. About 10 % of the measured wind profiles are available within the first 1000 m, which allows the investigation of the behavior with height of the two horizontal wind speed components. From the preliminary analysis of these vertical profiles, a variety of atmospheric and forcing conditions is distinguished; from a number of 10-min mean profiles the wind is observed to turn both anti- and clockwise more than  $50^\circ$ , likely indicating the influence of baroclinity.

**Keywords:** boundary-layer winds, FINO3, offshore, wind lidar, wind turning

## 1 Introduction

Observations of boundary-layer winds in the marine environment are scarce mainly because it is much more expensive to deploy instruments on meteorological towers offshore than over land. This is particularly problematic for regions and countries close to the North and Baltic Seas, as these two water masses strongly influence the weather and, therefore, the wind climate. Numerical weather prediction (NWP) mesoscale models, for example, are run using reanalysis products, which have been developed based on combining atmospheric models with observational assimilation systems. An in-depth description of one of the most used reanalysis products is given in DEE *et al.* (2011). Over land, the assimilation systems normally use wind observations from weather stations (mainly monitoring surface winds), radiosondes (which are inherently not highly accurate for wind speed measurements), and a limited number of wind profilers. Offshore, most wind-like observations come from satellites (primarily scatterometers), which provide estimates of the wind speed at 10 m above the surface only, with a somewhat high degree of uncertainty when compared to in-situ measurements (KARAGALI *et al.*, 2014). Therefore, the reanalysis is probably well 'tuned' for marine surface winds but it becomes highly uncertain for describing higher level winds as it mainly relies on the

atmospheric model. This sets a limit on the ability of NWP models to predict the wind climate in countries like Denmark, as the 'forcing' conditions lack observations of the marine vertical wind variability.

Further, harvesting of offshore wind energy continues its increasing rates (TPWIND, 2014) and as the installation costs of offshore turbines have dramatically increased, project developers want to use the largest turbines available. This nowadays means machines operating within the first 200 m of the atmosphere. Accurate information on the wind characteristics at these levels is therefore needed for power production and loads estimation. But as this information is generally non-existing, developers rely on micro- and mesoscale models for characterizing the wind conditions. Apart from the issues related to the reanalysis products used as forcing for the mesoscale models (described above), both types of models use parameterizations either of the vertical wind profile or of parameters of the planetary boundary layer (PBL) (evaluated with observations close to the ground), which account (erroneously or not at all) for the effect of parameters and phenomena such as the boundary-layer height (BLH) or baroclinity. PEÑA *et al.* (2008) showed the importance of the BLH for describing the marine vertical wind profile based on wind lidar observations up to 161 m, and although FLOORS *et al.* (2015) showed the effect of baroclinity on the vertical wind profile from land-based wind lidar observations, we anticipate that particularly close to the coasts, such

\*Corresponding author: Alfredo Peña, DTU Wind Energy, Risø campus, Technical University of Denmark, Roskilde, Denmark, e-mail: aldi@dtu.dk

effects are also considerable offshore. We are not aware of a microscale model, which takes into account the latter effects.

NWP PBL schemes are also known to have difficulties to account for the vertical wind shear (HU *et al.*, 2010; HAHMANN *et al.*, in review), which is of primary interest for wind power meteorology. Taking the above points in mind, the EU NORSEWInD project aimed to derive a numerical wind atlas for the north European Seas using a NWP model and established a observational network consisting mainly on wind lidars placed on platforms over the North and Baltic Seas for the evaluation of the NWP outputs. However, the wind speed observations, which were available within the turbine operating heights, lacked information about the state of the atmosphere and so it was difficult to evaluate the goodness of the model as atmospheric stability highly influences the vertical wind shear (PEÑA *et al.*, 2012). The “Tall wind” project, based on the above points, aimed to further explore the capabilities of the wind lidars by measuring winds in the entire PBL. Two onshore campaigns were already completed, and are described and analyzed in, e.g. FLOORS *et al.* (2013), GRYNING *et al.* (2013), PEÑA *et al.* (2014), and GRYNING *et al.* (2014). Here we describe the observations of a third and final campaign, which took place at the FINO3 offshore research platform in the German North Sea. This campaign is unique as such type of measurements, i.e. with that coverage, vertical resolution and accuracy, have not been performed before (from the authors’ knowledge), which allows us for a thorough evaluation of atmospheric models.

## 2 Definitions

Observations of the two horizontal wind speed components ( $u, v$ ) are here presented. The  $u$ -component is aligned with the mean wind speed vector at the first level used for the analysis and the  $v$ -component is that perpendicular to it, so at the first level  $v$  becomes zero. They are placed on a left-handed coordinate system; thus  $v$  increases and decreases when the wind vector turns clockwise and counterclockwise with height, respectively, which is what we expect in an ‘ideal’ boundary layer in the northern hemisphere. The horizontal wind speed magnitude is then estimated as  $U = (u^2 + v^2)^{1/2}$ .

When predicting the behaviour of the wind speed with height, the logarithmic wind profile has been shown to be valid within the surface layer under homogeneous, flat terrain, and neutral and barotropic conditions only (PEÑA and GRYNING, 2008; PEÑA *et al.*, 2010b). This is given as

$$U = \frac{u_*}{\kappa} \ln\left(\frac{z}{z_o}\right), \quad (2.1)$$

where  $u_*$  is the friction velocity,  $\kappa$  the von Kármán constant ( $\approx 0.4$ ),  $z$  the height, and  $z_o$  the surface roughness length.

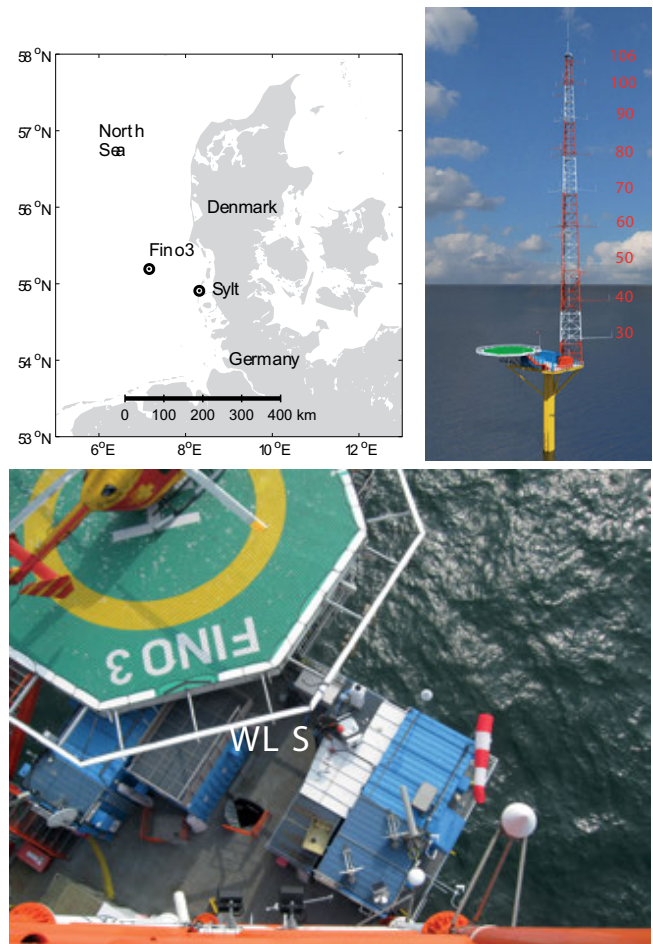


**Figure 1:** (Top left) location of the FINO3 research platform in the North Sea. (Top right) FINO3 research platform with the instrumentation levels in meters (© FuE-Zentrum FH Kiel GmbH, Graphic: Bastian Barton). (Bottom) location of the WLS70 wind lidar and the CL51 ceilometer (besides it) on the FINO3 platform.

## 3 Site and measurements

### 3.1 FINO3 offshore research platform

The FINO3 research platform is located in the German North Sea ( $55^\circ 11.7' \text{ N}$ ,  $7^\circ 9.5' \text{ E}$ ), 80 km off Sylt, Germany. The platform mainly consists of a 105-m triangular lattice tower,<sup>1</sup> a helipad, and containers on the platform’s base, which are used for, i.a. the storage, control and acquisition of data, and the deployment of instrumentation (see Figure 1). The ‘standard’ instruments at FINO3 are mounted on booms protruding the mast at  $105^\circ$ ,  $225^\circ$ , and  $345^\circ$  (see Tab. 1) and in order to minimize mast/boom distortion effects on the measurements the direction intervals  $345^\circ$ – $45^\circ$  and  $165^\circ$ – $225^\circ$ ,  $105^\circ$ – $165^\circ$  and  $285^\circ$ – $345^\circ$ , and  $225^\circ$ – $285^\circ$  and  $45^\circ$ – $105^\circ$ , respectively, can be selected (see Section 3.2).

Here we use the cup anemometer measurements at 106 and 100 m for the verification of the wind lidar, as

<sup>1</sup>all heights are referred to the level above mean sea level unless otherwise stated

**Table 1:** The instrumentation of the tower on the FINO3 research platform. Additional instrumentation is also deployed but these are the most relevant meteorological sensors.

Instrument	Boom location [°]	Height [m]
Cup anemometer	345	106, 100, 90, 80, 70, 60, 50, 40, and 30
Cup anemometer	105	90, 70, and 50
Cup anemometer	225	90, 70, and 50
Sonic anemometer	225	100 and 60
Wind vane	105	100 and 28
Temperature and humidity sensors	105	95, 55, and 29
Precipitation and air pressure sensors	105	94 and 23
Radiation sensor	105	23

these are the cups closest to the first wind lidar observation, and those at 100, 60, and 30/28 m for the wind profile analysis, as wind direction information is also available at these levels. During the wind lidar campaign, most data from the mast at the FINO3 platform are available until the 31 March 2014. Particularly the 106-m cup measurements are only available until the 31 December 2013. Data from the tower are only available in 10-min averages.

### 3.2 Wind lidar

A WindCube pulsed wind lidar (WLS70) from Leosphere was installed over the containers on the FINO3 platform on the 23rd of August 2013 and run until the 6th of October 2014. This wind lidar measures the line-of-sight velocity at four azimuthal positions each 90° with an inclination from the zenith of 15°. The measurement volume extends  $\approx 60$  m at the line-of-sight. The three wind speed components are derived every  $\approx 10$  s (the time it takes to move to the next azimuthal position) assuming horizontal flow homogeneity, and these raw data together with the 10-min averages are stored in a database. The system is capable of measure winds from 100 up to 2000 m every 50 m (these are above-lidar heights) depending on the aerosol content and carrier-to-noise ratio (CNR).

The wind lidar observations presented here correspond to the period between 23 August 2013 and 26 June 2014. All wind lidar observations are filtered so that all measurements within the 10-min are valid and readily available. This mainly implies that all the raw data must be valid within the 10-min period.

As an overview of the wind lidar campaign, Figure 2-left illustrates the wind speed rose measured by the wind lidar at 124.5 m when the wind lidar data are only filtered for this particular level (average 10-min CNRs higher than  $-22$  dB are always used as filter for this study). This wind rose mainly describes the wind climate at FINO3 without accounting a part of the summer period. Predominant winds, as expected, are southwest, which is a priori a good sign as most of these directions are less distorted at the instruments on the 345° booms, i.e. the ‘row’ of cups from 30–106 m. However, if wind lidar data from the first 19 levels are used (i.e. up to 1024.5 m), due to CNR filtering and data availability

the wind rose for such profiles changes and the predominant winds become those from northwest. Interesting to note is the observed high wind speed range (up to  $45 \text{ m s}^{-1}$ ), which is partly a result of storm periods at the end of 2013 (see Section 4.3). As illustrated most of the wind speeds observed at FINO3 at 124.5 m are within the range  $10\text{--}15 \text{ m s}^{-1}$ .

### 3.3 Ceilometer

A CL51 Vaisala ceilometer was also deployed on the FINO3 platform 1 m from the wind lidar (see Figure 1-bottom) and has been running for the same period. The instrument is also a pulsed lidar but it does not measure the Doppler frequency shift between emitted and received light but the volume aerosol backscatter coefficient. The system was setup so that the backscatter is retrieved every 10 m from 10 up to 7700 m (these are above-ceilometer heights) at a resolution of  $\approx 16$  s.

## 4 Results

### 4.1 Wind lidar reliability

The total amount of 10-min data measured by the wind lidar at the first measurement height is 42686, a remarkable number given that 44208 10-min are the total data potential that could be observed during the period here analyzed (the system only stopped working during 8 days due to a general power cut at the platform). Figure 3-left shows the availability of wind lidar measurements per height for different minimum CNRs (average CNR over the 10-min) at FINO3. The shape of the curves peak nearly at the same height ( $\approx 300$  m) because this is the focused distance of the wind lidar and so they look similar to those relating the CNR variation with focused distance described in [SONNENSCHNIG and HERRIGAN \(1971\)](#). Although the data availability highly decreases with height above 400 m, for such type of pulsed system this is a good performance; the amount of available data is slightly higher compared to that of the two previous campaigns at onshore sites: a coastal site in western Denmark and at a rural site close to Hamburg ([BRÜMMER et al., 2012](#); [FLOORS et al., 2015](#)). At the coastal site, the percentage of data where  $\text{CNR} > -22$  dB at  $\approx 1000$  m was 9 % and at FINO3 11 %.



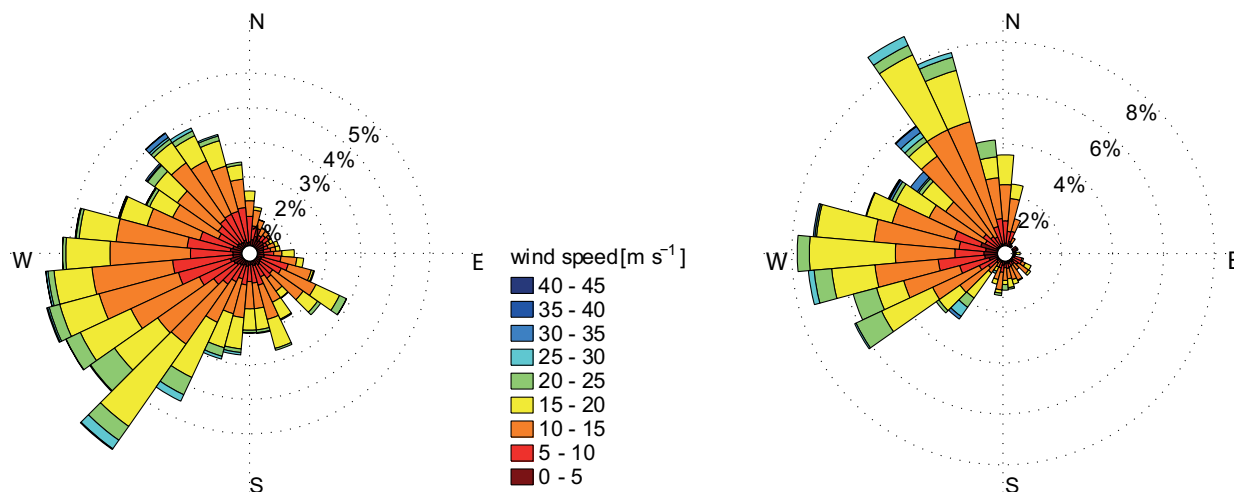


**Figure 2:** (Left) wind rose measured by the wind lidar at 124.5 m at the FINO3 platform. (Right) similar as the left frame but only for data completely available up to 1024.5 m.

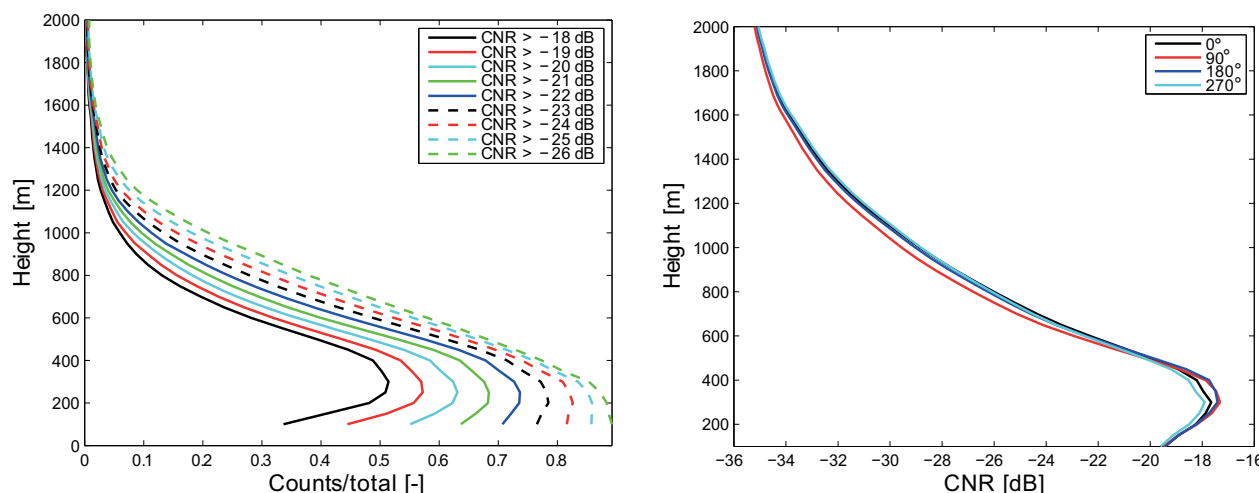


**Figure 3:** (Left) wind lidar availability as function of height (above lidar) and minimum 10-min mean CNR. (Right) ensemble average of 10-min mean CNRs as function of height (above lidar) and per azimuthal position of the lidar beam at the FINO3 platform.

Figure 3-right shows the behavior of the ensemble average of the 10-min mean CNRs with height for each of the wind lidar azimuthal positions when measuring at FINO3 (we use a minimum CNR of  $-50$  dB for the raw data). As for the wind lidar availability, the CNR curves for the four azimuthal positions peak at the focused distance of  $\approx 300$  m and their very close behaviour suggests no systematic interference of hard targets or any other source of beam degradation.

## 4.2 Wind lidar verification

The use of a minimum mean CNR-value of  $-22$  dB for the 10-min data of this specific wind lidar was recommended in Peña et al. (2013) and used in Floors et al. (2013), Peña et al. (2014), and Floors et al. (2015) successfully. Figure 4 illustrates comparisons of the wind lidar 10-min mean wind speed and direction observations at the first level (124.5 m) against cup anemometer measurements at 106 and 100 m and the wind vane at

100 m on the tower at FINO3 (only ‘free’ directions are used for the wind speed comparisons, see Section 3.1). The wind lidar measurements are filtered so that the 10-min mean CNR values are higher than  $-22$  dB. Both types of observations are very well correlated at the two heights; the Pearson’s linear correlation coefficients  $R^2$  are close to 1 as found in Peña et al. (2014) for the coastal site. The results of the intercomparison suggest that the wind speed at 106 and 100 m are about 2 and 3 % lower than that at 124.5 m, which are close (but higher than) to what is expected when assuming the wind speed follows the logarithmic wind profile, i.e. Eq. (2.1) with  $z_o = 0.0002$  m (the directions analyzed are nevertheless not completely “free” of mast/boom distortion effects and so such effects can explain a slight part of the difference).

For the wind direction it is noticed a systematic  $11.7^\circ$  difference. The offset would not be systematic, if it was due to the ‘natural’ turning of the wind with height and so this reflects that either the vane or the wind lidar

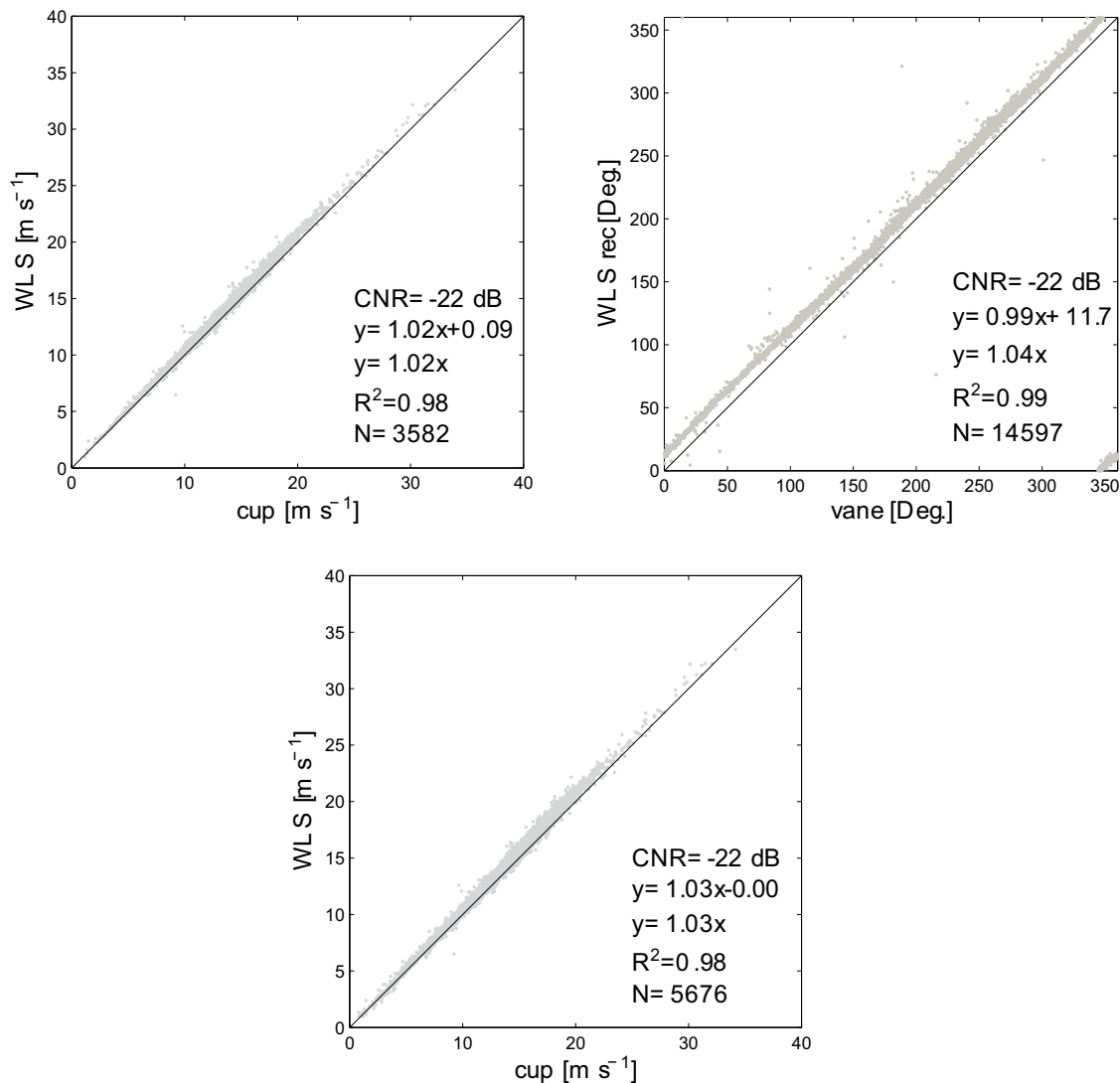


**Figure 4:** Scatter plots of the observed 10-min mean wind speed and direction from the wind lidar at 124.5 m and the cup anemometers and vanes at the FINO3 platform. (Upper left) wind lidar and 106-m cup anemometer wind speed, (upper right) wind lidar and 100-m vane, and (bottom) wind lidar and 100-m cup.

are misaligned with the north (or both). Analysis of the directions measured by the sonic at 60 m and the vane at 28 m (not shown) reveals no systematic offset when compared to the vane at 100 m, which means that the tower instruments were aligned with the same north. The direction offset of the lidar can therefore be easily adjusted to match the tower-based direction (or viceversa) and it will be the same for all observed levels (the offset is rather small so it does not matter whether the wind lidar or the tower directions are corrected).

### 4.3 Wind evolution

The relatively high availability of wind lidar data within the first  $\approx 600$  m provides the opportunity to investigate the evolution of the marine boundary-layer winds. On the 5th of December 2013, a cyclone (named Xaver in Germany) passed by FINO3 and the wind lidar was able to measure 10-min mean wind speeds higher than  $40 \text{ m s}^{-1}$  within the layer 400–600 m (wind speeds above

$60 \text{ m s}^{-1}$  were observed in the 10-s raw data within the same layers).<sup>2</sup> The wind lidar did not only ‘survive’ the storm (and some others occurring during the period October 2013–January 2014) but detected interesting features in the structure of it (see Figure 5). First, during the whole day winds were always above  $15 \text{ m s}^{-1}$ . Second, there are a good number of records, particularly from 12:00 to 18:00 local standard time (LST), where profiles with wind speeds higher than  $40 \text{ m s}^{-1}$  are observed within the first  $\approx 800$  m. It can also be seen that between 06:00 to 13:30 LST the wind was from the south-southwest ( $\approx 180^\circ$ ) and at the end of this period it abruptly changed to  $230^\circ$  and within a 2-hr period it turned  $90^\circ$  more north west.

According to LEIDING et al. (2014), the peak of Xaver was at 18 UTC; during the 5th of December and after 03:00 UTC, they recorded 10-min mean wind speeds

<sup>2</sup>this is probably the fastest atmospheric ‘gust’ recorded by a wind lidar

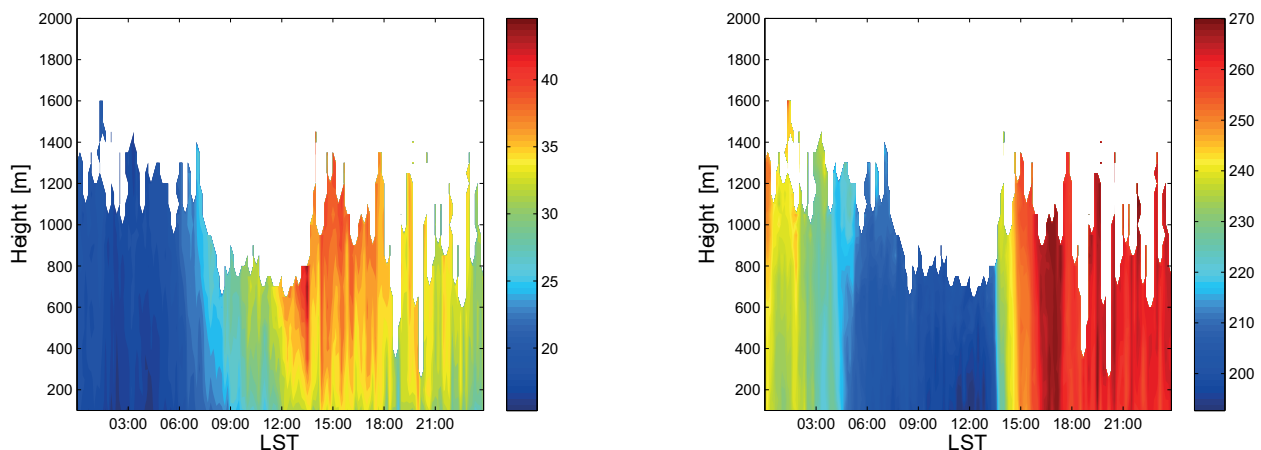


**Figure 5:** (Left) wind speed and (right) direction observed by the wind lidar at the FINO3 platform during cyclone Xaver on 05 December 2013. The colorbars are in  $\text{m s}^{-1}$  for the wind speed and in deg. for the direction. The height in both plots is that above the wind lidar.

higher than  $15 \text{ m s}^{-1}$  at 103 m with the highest value of  $38 \text{ m s}^{-1}$ , and with a maximum 1-s gust of  $49.2 \text{ m s}^{-1}$  at the FINO1 offshore platform (45 km north of Borkum, Germany). In agreement with our wind lidar observations, they also measured a rapid change of wind direction after 13:30 UTC, where the wind turned from west-southwest to west continuing to northwest within a 10-min period. DEUTSCHLÄNDER et al. (2013) provides an overview of the peak gusts and sustained wind records of Xaver from a network of weather stations in northern Germany and surrounding countries.

#### 4.4 Aerosol backscatter

The ceilometer installed at the platform allows the investigation of features related to turbulent structures in the atmosphere, otherwise not observed by the meteorological tower at FINO3, because this particular instrument is rather sensitive and can retrieve a detailed profile of the aerosol backscatter intensity. However, at FINO3 clouds are very frequent (much more than at the coastal site in Denmark), which increases the complexity for further analysis of the ceilometer outputs as the backscatter intensity retrieved from cloud layers is much higher than that under clear sky conditions.

In Figure 6-left we illustrate a typical backscatter signal at FINO3 (from 15 November 2013), where a limit of  $250 \text{ m}^{-1} \text{ sr}^{-1} \times 10^{-5}$  on the intensity is used for plotting purposes (otherwise the layers below the clouds will be hidden). There are two cloud layers from 00:00 to 12:00 LST (at  $\approx 1200$  and  $600$  m) and even some rain (brown patches between the two layers), which was also recorded by the two precipitation sensors at FINO3. The backscatter information can be used to derive the BLH (EMEIS and SCHÄFER, 2006; EMEIS et al., 2008), which can be used, i.a. for the analysis of wind profiles (GRYNING et al., 2007; PEÑA et al., 2010a). In this particular example, the height of the lowest cloud layer is most probably also a good estimation of the BLH.

PEÑA et al. (2013) demonstrated that the WLS70 wind lidar can also be used for detecting BLHs. Figure 6-right illustrates the observed CNR for the same day and, as expected, the CNR is highest where the backscatter intensity is also highest. The advantage of using the wind lidar's CNR values over the ceilometer's backscatter signal is that the values under cloud conditions do not increase that dramatically and so gradient or idealized-profile methods for BLH detection might be easy to implement and robust.

#### 4.5 Boundary-layer wind profiles

The range and quality of observations of this wind lidar results in a unique dataset to study the vertical wind profiles and the turning of the wind with height in the marine environment. As a preliminary overview of the data, we select all 10-min wind lidar profiles where all levels within the range 100–1000 m above lidar are available with  $\text{CNR} > -22 \text{ dB}$ . The two horizontal wind speed components are here rotated so that  $u = U$  at the first wind lidar level. The selection results in 3164 10-min mean wind profiles and, as illustrated in Figure 7, they are most likely the result of a variety of atmospheric and forcing conditions as wind speeds are observed in the range  $\approx 0\text{--}35 \text{ m s}^{-1}$  at the first level.

Focusing on the behavior of the  $u$ -component, it is noticed a good number of profiles where the values become negative at  $\approx 300$  m, most probably indicating the influence of baroclinity. Such influence can also be observed on the  $v$ -component, where a similar number of profiles show rather high negative values; positive values indicate that the wind turns clockwise (as expected in the barotropic northern atmosphere) and so baroclinity can be the cause of the counterclockwise turning. The maximum absolute  $v$ -values are  $\approx 10 \text{ m s}^{-1}$ , which means a relative turning of the wind of  $\approx 45^\circ$  (assuming similar absolute values for  $u$ ) within the analyzed range.

Some of these profiles (highlighted in blue in Figure 7) correspond to a 1.5-hr period in the afternoon of

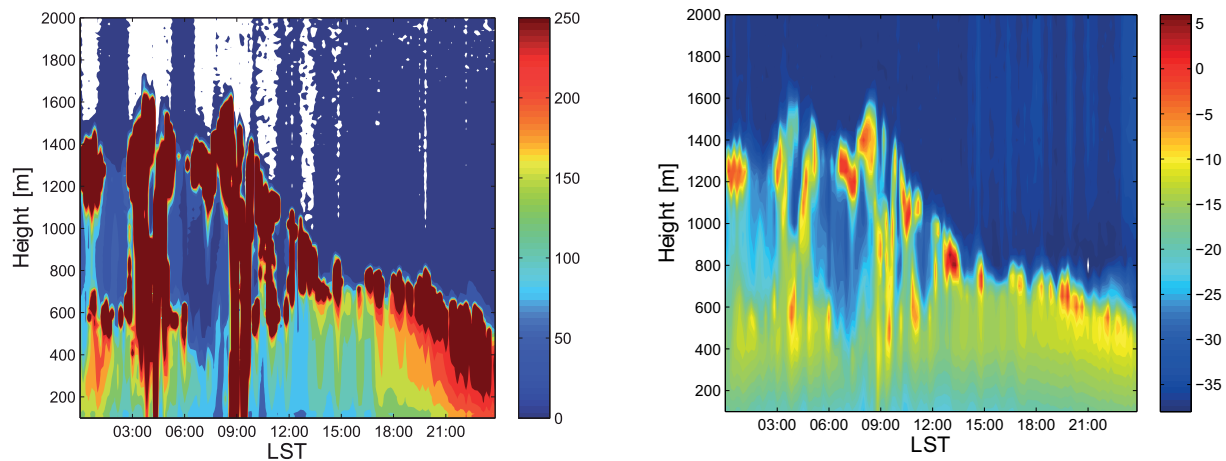


**Figure 6:** (Left) volume aerosol backscatter coefficient and (right) carrier-to-noise ratio (CNR) measured by the ceilometer and the wind lidar, respectively, during 15 November 2013 at the FINO3 platform. The colorbars indicate, respectively, the backscatter intensity in  $\text{m}^{-1} \text{sr}^{-1} \times 10^{-5}$  and CNR in dB. The height in both plots is that above the wind lidar.

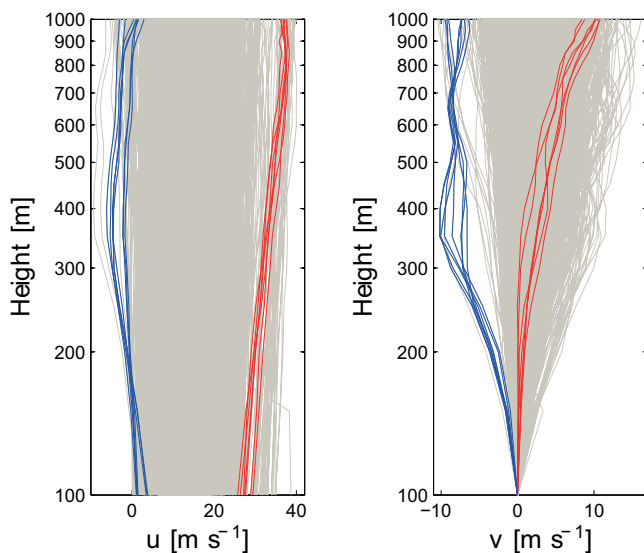


**Figure 7:** Vertical profiles of the 10-min mean horizontal wind speed components observed in the range 100–1000 m by the wind lidar at the FINO3 platform. The height is that above the wind lidar. The blue and red profiles correspond to two particular cases (see text for details).

the 26th of April 2014. During this period, the atmosphere was stable (the difference in the potential temperature between the 55 and 29 m levels was 1.29 K), which partly explains the high shear in the profiles. Further, using mesoscale model outputs, the thermal wind can be estimated from the geopotential horizontal gradients (refer to [Peña et al. \(2014\)](#) and [Floors et al. \(2015\)](#) for details about the methodology to derive large-scale winds from numerical weather prediction model outputs). The maximum thermal wind within the first 966 m is  $\approx 5 \text{ m s}^{-1}$ , which further explains both the high wind shear and the counterclockwise turning.

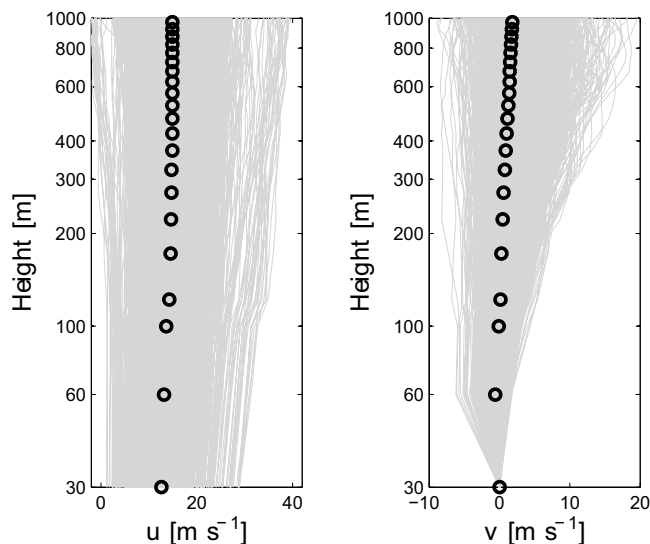
Other profiles, such as those highlighted in red in Figure 7, follow a nearly linear behavior in this semi-

logarithmic plot, as shown for the  $u$ -component. These profiles correspond to a 1-hr period in the morning of the 15th of February 2014, where the potential temperature difference was only 0.20 K, which indicates that the atmosphere was probably near neutral, also explaining the very high observed wind speeds. The maximum thermal wind for these profiles is estimated to be only  $\approx 1.50 \text{ m s}^{-1}$ .

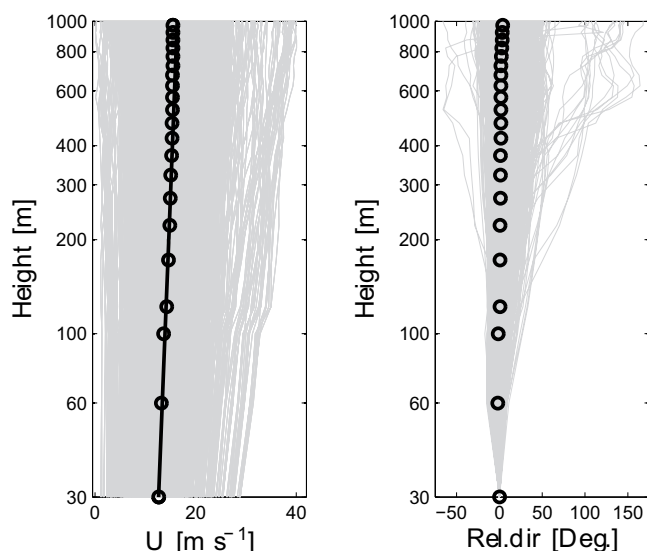
As BLHs can be lower than 100 m, it is important to ‘extend’ the wind lidar profiles with those from the cup anemometers on the tower at FINO3. For this particular analysis, we are interested on the behavior of both wind speed components with height and so we need to select levels at the tower where both wind speed and direction information are available, which leaves us with the 30, 60, and 100 m levels (for the 60-m level we use the wind direction from the sonic at 60 m and for the other two the wind vanes at 28 and 100 m). Figure 8 illustrates the 1574 10-min mean wind profiles that result from matching the tower and wind lidar observations. The directions from the wind lidar were rotated  $10^\circ$  based on the comparison with the vanes’ direction. The number of wind profiles is much lower than only using wind lidar data because the tower data is only available until 31 March 2014. Since we use the 30, 60, and 100 m levels, where only one cup anemometer is available, some of these profiles might be highly distorted by the wake of the mast; however for this preliminary profile analysis this is not important. It can also be noticed, from the  $v$ -profiles, that there might be an offset of the 28-m vane with respect to the other direction measurements because the  $v$ -profiles mostly decrease from 30 to 60 m, implying a backing of the wind (counterclockwise turning). However, the 28-m vane is close to the helipad level and is mounted on the  $105^\circ$  boom, which might face high flow distortion from both the helipad and the mast.

Figure 9 illustrates for the same matched wind lidar/tower dataset the profiles of horizontal mean wind speed magnitude and relative direction. As shown, the





**Figure 8:** Vertical profiles of the 10-min mean horizontal wind speed components observed in the range 30–1000 m by the wind lidar and the tower instruments at the FINO3 platform. The ensemble average of the profiles is shown in black circles



**Figure 9:** Vertical profiles of the 10-min mean horizontal wind speed magnitude (left) and relative direction (right) observed in the range 30–1000 m by the wind lidar and the tower instruments at the FINO3 platform. The ensemble average of the profiles is shown in black circles and the prediction using the logarithmic wind profile in the solid black line.

ensemble average of all 10-min mean  $U$ -profiles is very close to logarithmic and only for illustrative purposes we plot the logarithmic wind profile, which fits rather well the ensemble average of observations (we find  $u_*$  so that Eq. (2.1) matches the wind speed at 30 m using  $z_o = 0.0002$  m). The explanation of this good agreement does not have to do with the ability of the logarithmic wind profile to predict marine winds but because the ensemble average of observations tends to show a profile

close to that of neutral stability conditions; it is actually closer to slightly unstable conditions as most of the matched data are from November records. These misleading ‘neutral’ wind profiles were already discussed in Peña et al. (2009) but only up to 161 m. Interestingly, some profiles of relative direction indicate wind veering higher than  $100^\circ$ , as well as some wind backing of  $50^\circ$ , both most probably due to baroclinity. The ensemble average, however, only shows a wind veering of  $4.25^\circ$  within the first 1000 m.

## 5 Conclusions and perspectives

Measurements of a nearly 1-yr campaign performed at the FINO3 research platform combining tower and wind lidar observations are presented. The wind lidar, a pulsed system that can measure vertical wind profiles up to 2000 m, showed a high reliability and data availability. At the first height of wind lidar measurements (124.5 m) the data availability over the data potential is  $\approx 97\%$ ; this decreases with height above 300 m but a good number of profiles are still measured up to 1000 m.

The wind lidar shows very good agreement and correlation when compared to the tower measurements of wind speed and direction at FINO3. The wind lidar is able to perform observations under very high wind speed conditions, namely, during the Xaver storm, 10-min and 10-s wind speed measurements above 40 and  $60 \text{ m s}^{-1}$  were recorded. This particular wind lidar can also provide a picture of the behaviour of the BLH, since as we show, the CNR measurements are closely related to the aerosol backscatter from ceilometer observations also performed at the platform.

From the analysis of vertical profiles of the two horizontal wind speed components, we can identify a number of atmospheric stability and forcing conditions as winds are observed in a wide range of speeds, wind shears and to turn clockwise and counterclockwise; a number of 10-min winds are turning more than  $45^\circ$  in both directions. The logarithmic wind profile is found to predict well the ensemble average wind profile of observations up to 1000 m, although the ensemble atmospheric conditions are considered to be slightly unstable.

For the wind profile analysis, we selected cup anemometers that might be distorted by the mast wake. We plan in the future to investigate how to best extend the wind lidar profiles with the tower measurements as we anticipate further analysis of the FINO3 campaign focusing on:

- atmospheric stability influence on both vertical wind shear and turning of the wind conditions.
- influence of baroclinity on both wind speed and turning of the wind conditions.
- prediction of “tall” wind profiles, of both horizontal wind speed components, with numerical models of the micro- and macroscale types.

- detection of the marine BLH with the wind lidar and ceilometer and comparison with simulated BLHs from mesoscale models
- and vertical profiles of Weibull distribution parameters and comparison with results from numerical modelling.

## Acknowledgements

The authors thank the Danish Council for Strategic Research for funding of the “Tall Wind” project (No. 2104-08-0025) and the German Federal Ministry for the Environment, Nature Conservation and Nuclear Safety (BMU) for sharing the FINO3 data. Fraunhofer IWES and DONG Energy A/S are also acknowledged for the support of the FINO3 campaign.

## References

- BRÜMMER, B., I. LANGE, H. KONOW, 2012: Atmospheric boundary layer measurements at the 280 m high Hamburg weather mast 1995–2011: mean annual and diurnal cycles. – *Meteorol. Z.* **21**, 319–335.
- DEE, P.D., S.M. UPPALA, A.J. SIMMONS, P. BERRISFORD, P. POLI, S. KOBAYASHI, U. ANDRAE, M.A. BALMASEDA, G. BALSAMO, P. BAUER, P. BECHTOLD, A.C.M. BELJAARS, L. VAN DE BERG, J. BIDLOT, N. BORMANN, C. DELSOL, R. DRAGANI, M. FUENTES, A.J. GEER, L. HAIMBERGER, S.B. HEALY, H. HERSBACH, E.V. HÖLM, L. ISAKSEN, P. KÄLLBERG, M. KÖHLER, M. MATRICARDI, A.P. McNALLY, B.M. MONGE-SANZ, J.-J. MORCRETTE, B.-K. PARK, C. PEUBEY, P. DE ROSNAY, C. TAVOLATO, J.-N. THÉPAUT, F. VITART, 2011: The ERA-Interim reanalysis: configuration and performance of the data assimilation system. – *Quart. J. Roy. Meteor. Soc.* **137**, 553–597.
- DEUTSCHLÄNDER, T., K. FRIEDRICH, S. HAESELER, C. LEFEBVRE, 2013: Severe storm XAVER across northern Europe from 5 to 7 December 2013. – Technical report, Deutscher Wetterdienst (DWD), 19 pp.
- EMEIS, S., K. SCHÄFER, 2006: Remote sensing methods to investigate boundary-layer structures relevant to air pollution in cities. – *Bound.-Layer Meteor.* **121**, 377–385.
- EMEIS, S., K. SCHÄFER, C. MÜNKEL, 2008: Surface-based remote sensing of the mixing-layer height – a review. – *Meteorol. Z.* **17**, 621–630.
- FLOORS, R., C.L. VINCENT, S.-E. GRYNING, A. PEÑA, E. BATCHVAROVA, 2013: The wind profile in the coastal boundary layer: wind lidar measurements and numerical modelling. – *Bound.-Layer Meteor.* **147**, 469–491.
- FLOORS, R., A. PEÑA, S.-E. GRYNING, 2015: The effect of baroclinicity on the wind in the planetary boundary layer. – *Quart. J. Roy. Meteor. Soc.* **141**, 619–630.
- GRYNING, S.-E., E. BATCHVAROVA, B. BRÜMMER, H. JØRGENSEN, S. LARSEN, 2007: On the extension of the wind profile over homogeneous terrain beyond the surface layer. – *Bound.-Layer Meteor.* **124**, 251–268.
- GRYNING, S.-E., E. BATCHVAROVA, R. FLOORS, 2013: A study on the effect of nudging on long-term boundary-layer profiles of wind and weibull distribution parameters in a rural coastal area. – *J. Applied Meteor. Climatol.* **52**, 1201–1207.
- GRYNING, S.-E., E. BATCHVAROVA, R. FLOORS, A. PEÑA, B. BRÜMMER, A.N. HAHMANN, T. MIKKELSEN, 2014: Long-term profiles of wind and weibull distribution parameters up to 600 m in a rural coastal and an inland suburban area. – *Bound.-Layer Meteor.* **150**, 167–184.
- HAHMANN, A.N., C. VINCENT, A. PEÑA, J. LANGE, C.B. HASAGER, in review: Wind climate estimation using WRF model output: method and model sensitivities over the sea. – *Int. J. Climatol.* DOI:10.1002/joc.4217.
- HU, X.-M., J.W. NIELSEN-GAMMON, F. ZHANG, 2010: Evaluation of three planetary boundary layer schemes in the WRF model. – *J. Appl. Meteor. Climatol.* **49**, 1831–1844.
- KARAGALI, I., A. PEÑA, M. BADGER, C.B. HASAGER, 2014: Wind characteristics in the North and Baltic Seas from QuikSCAT satellite. – *Wind Energy* **17**, 123–140.
- LEIDING, T., B. TINZ, G. ROSENHAGEN, C. LEFEBVRE, S. HAESELER, S. HAGEMANN, I. BASTIGKEIT, D. STEIN, P. SCHWENK, S. MÜLLER, O. OUTZEN, K. HERKLOTZ, F. KINDER, T. NEUMANN, 2014: Meteorological and oceanographic conditions at the FINO platforms during the severe storms CHRISTIAN and XAVER. – *DEWI Magazin* **44**, 16–25.
- PEÑA, A., S.-E. GRYNING, 2008: Charnock’s roughness length model and non-dimensional wind profiles over the sea. – *Bound.-Layer Meteor.* **128**, 191–203.
- PEÑA, A., S.-E. GRYNING, C.B. HASAGER, 2008: Measurements and modelling of the wind speed profile in the marine atmospheric boundary layer. – *Bound.-Layer Meteor.* **129**, 479–495.
- PEÑA, A., C.B. HASAGER, S.-E. GRYNING, M. COURTNEY, I. ANTONIOU, T. MIKKELSEN, 2009: Offshore wind profiling using light detection and ranging measurements. – *Wind Energy* **12**, 105–124.
- PEÑA, A., S.-E. GRYNING, C.B. HASAGER, 2010a: Comparing mixing-length models of the diabatic wind profile over homogeneous terrain. – *Theor. Appl. Climatol.* **100**, 325–335.
- PEÑA, A., S.-E. GRYNING, J. MANN, 2010b: On the length-scale of the wind profile. – *Quart. J. Roy. Meteor. Soc.* **136**, 2119–2131.
- PEÑA, A., T. MIKKELSEN, S.-E. GRYNING, C.B. HASAGER, A. HAHMANN, M. BADGER, I. KARAGALI, M. COURTNEY, 2012: Offshore vertical wind shear: Final report on NORSEWInD’s work task 3.1. – DTU Wind Energy-Report-0005(EN), DTU Wind Energy.
- PEÑA, A., S.-E. GRYNING, A.N. HAHMANN, 2013: Observations of the atmospheric boundary layer height under marine upstream flow conditions at a coastal site. – *J. Geophys. Res. Atmos.* **118**, 1924–1940.
- PEÑA, A., R. FLOORS, S.-E. GRYNING, 2014: The Høvsøre tall wind-profile experiment: a description of wind profile observations in the atmospheric boundary layer. – *Bound.-Layer Meteor.* **150**, 69–89.
- SONNENSCHNEIN, C.M., F.A. HERRIGAN, 1971: Signal-to-noise relationships for coaxial systems that heterodyne backscatter from the atmosphere. – *Appl. Opt.* **10**, 1600–1604.
- TPWIND, 2014: Strategic Research Agenda/Market Deployment Strategy (SRA/MDS). – Technical report, European Wind Energy Technology Platform, Brussels.